ADVANCED STRUCTURE ANALYSIS OF HARD MAGNETIC Al-Mn ALLOYS

P. Švec, I. Janotová, P. Švec Sr., M. Mihalkovič

Institute of Physics, Slovak Academy of Sciences, Bratislava, Slovakia,
fyzipsvc@savba.sk

Received: 15 May 2017; accepted: 25 May 2017

1. Introduction

The need for rare-earth free or at least rare-earth-poor hard magnets emphasizes the focus on alloy systems based on Fe-Pt, Co-Pt, Bi-Mn and Al-Mn [1]. In Al-Mn alloy the main issue is, alongside with the development of suitable technology to obtain $Al_{45}Mn_{55}$ alloy with sufficient purity and in reasonable quantity, the formation of the optimal amount of the ferromagnetic τ-AMnl phase. For practical reasons and possible production upscale, metallurgical preparation of a master alloy and its rapid quenching into ribbon or flake form with subsequent suitable thermal treatment seems among the most suitable.

As shown in our previous work [2], as-quenched ribbon contains a mixture of ε- and τ-phases, the ε-phase being a majority phase created in the process of rapid quenching. Isothermal annealing in the temperature region between 650 – 713 K for several tens of minutes has been shown to lead to transformation of the ε-phase into τ-AlMn phase which already exhibits acceptable hard magnetic properties, especially magnetic coercivity and energy product.

The structure of both types of $Al_{45}Mn_{55}$ phases has been crystallographically investigated previously [3]. However, experimental verification of the validity of atomic scale models has not been verified yet. In addition, the process controlling the transformation from of ε- to τ-phase has not been clarified and it is not known whether the process is of the martensitic type or whether the transformation takes place by nucleation and growth of the forming ε-phase [4]. The τ-phase formation has also been assumed be accompanied by micro-twinning associated with stress relaxation at the growth front [5].

We shall try to investigate the local chemical order of the phases present in rapidly quenched $Al_{45}Mn_{55}$ in as-quenched state and after thermal treatment and to assess the issue of controlling mechanisms of ε- to τ-phase transformation by *in-situ* transmission electron microscopy.

2. Experimental

The $Al_{45}Mn_{55}$ samples in form of ribbon 3 mm wide and ~17 mm thick were prepared by planar flow casting (PFC) method. The ribbons were cast from master alloy manufactured in induction furnace from Al and Mn components with purity better then 99.95% (electrolytic). The structure of the master alloy, as-quenched and samples isothermally annealed in vacuum at 713 K for 1 hour was preliminarily investigated by X-ray diffraction (XRD) using Bruker D8 Advance diffractometer (Cu$K\alpha$ radiation) [6]. Conventional and *in-situ* transmission electron microscopy (TEM) has been performed using JEOL 2000FX at 200 kV with Gatan 652 heating holder and temperature controller system. Chemically resolved structure analysis on atomic scale has been performed using aberration corrected FEI Titan Themis 300 in scanning transmission electron microscopy (STEM) mode equipped with electron energy loss spectroscopy (EELS) and energy dispersive spectroscopy (EDS), accelerating voltage was 200kV. Sample for microscopy analyses were prepared by Ar ion beam milling using low energy ion mill (Fischione Model 1010). Samples for STEM observations have been cleaned in gentle plasma (Evactron XEI 25e).

3. Results and discussion

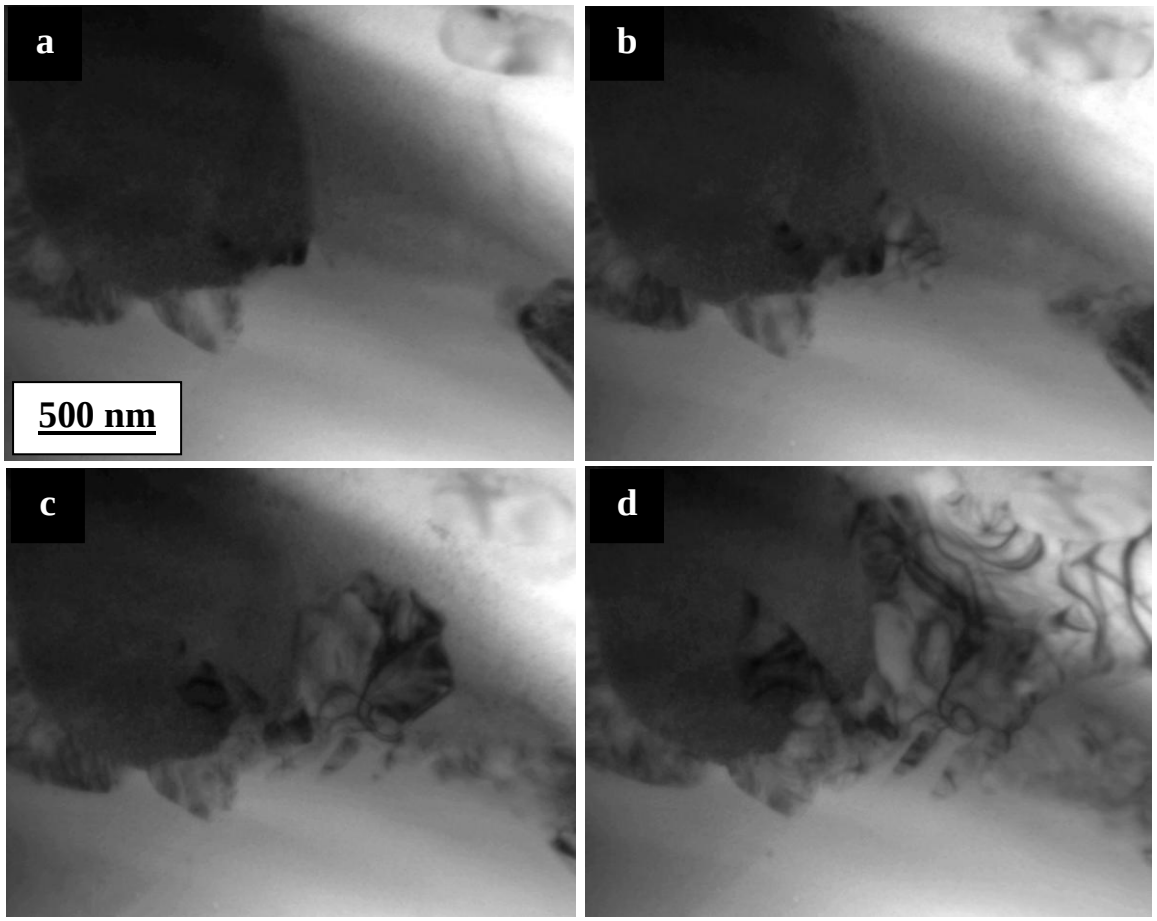

Fig. 1: *In-situ TEM micrographs of transformation process of ε- to τ-AlMn phase annealed at 713 K for (a) 1 min, (b) 10 min, (c) 30 min and (d) 60 min.*

In-situ TEM at 713 K (Fig. 1) shows that the structure is composed mainly of the ε-phase seen in image (a) as light gray matrix; contrasting grain at top left and middle right side of the image are the same phase, however, with different orientation as verified by electron diffraction (not shown). Image (b) shows that after a short time a new particle starts growing from the contrasting grain towards the right side of the image, along the grain boundary of the two light gray grains at the bottom and top of the image. With increasing time - image (c) - the grain of the new phase grows in flower-like shapes in all directions and additional grains appear. Prolonged annealing - image (d) – leads to further intense growth of the same phase into both grains of the original light-gray phase. Electron diffraction pattern (not shown) has identified the newly formed phase as τ-AlMn. The overall character of the process over time shows that growth starts preferentially at the existing grain boundaries of the ε-phase without formation of significant facets or defects on the boundaries or in the volume of the new phase.

Detailed structure characterization of the as-quenched state is presented in Fig. 2 and 3, where atomically resolved HAADF (high angle annular dark field) STEM micrographs are shown. EDS map of Mn alpha line suggest inhomogeneous Mn distribution across the ε-AlMn lattice, Fig 2. This is also seen as intensity variation among Al/Mn columns in the corresponding HAADF STEM micrograph. It is worth to note that the ε-AlMn grains are rather large (~10μm), irregular in shape and filled with inclusions. The whole ε-AlMn matrix

(dark grey area) acts as a coherently diffracting domain even filled with inclusions (white/black), Fig. 3. The inclusions do not cause any abnormal twinning effects or unusual microstructural strain to the ε-AlMn matrix. On the other hand, the inclusions exhibit severe twinning and induced strain as visualized with enhanced contrast variations. To confirm this, a strain sensitive DF (dark field) STEM detector (collection angles 23-98mrad) was used to visualize the strain induced contrast.

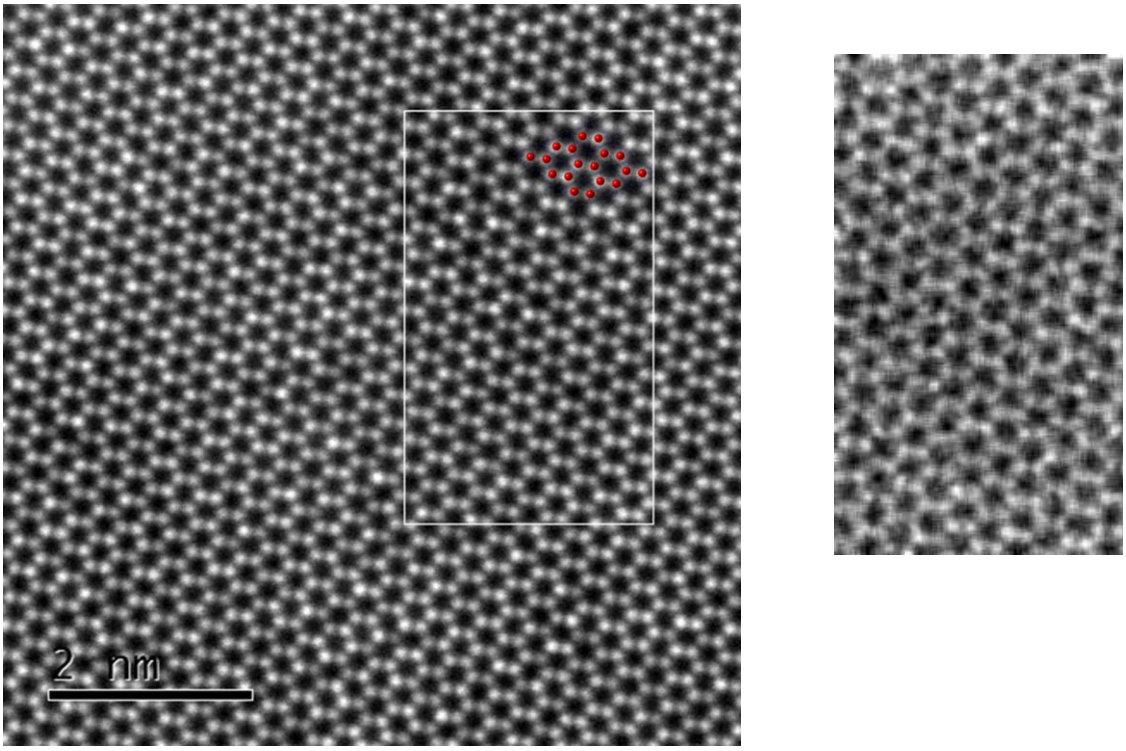

Fig. 2: *HAADF STEM micrograph of matrix region (ε-AlMn, [001] viewing direction) in the as-quenched state together with corresponding atomic model (3x3 unit cell, Al/Mn occupying the same columns). Atomically resolved Mn-kAlpha EDS map right.*

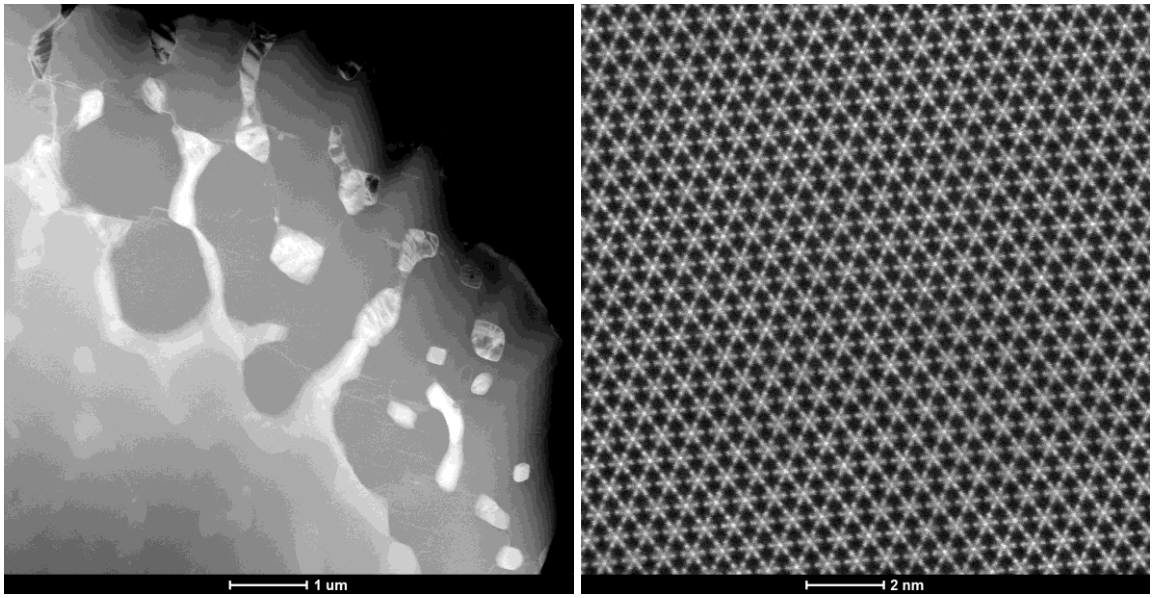

Fig 3: *DF STEM micrograph of the as-quenched state (left), HAADF STEM micrograph of the ε –AlMn grain inclusion (right).*

After the heat treatment/*in-situ* experiment the ε-AlMn transforms to τ-AlMn. This is expected behavior; however, the grain inclusion is being intact and does not participate on the ε to τ-AlMn transition. Evidence for this is the *in-situ* experiment, inclusion in top right corner of Fig. 1 and in detail in Fig. 4. The presence of this inclusion type phase is also observed in conventionally annealed bulk samples.

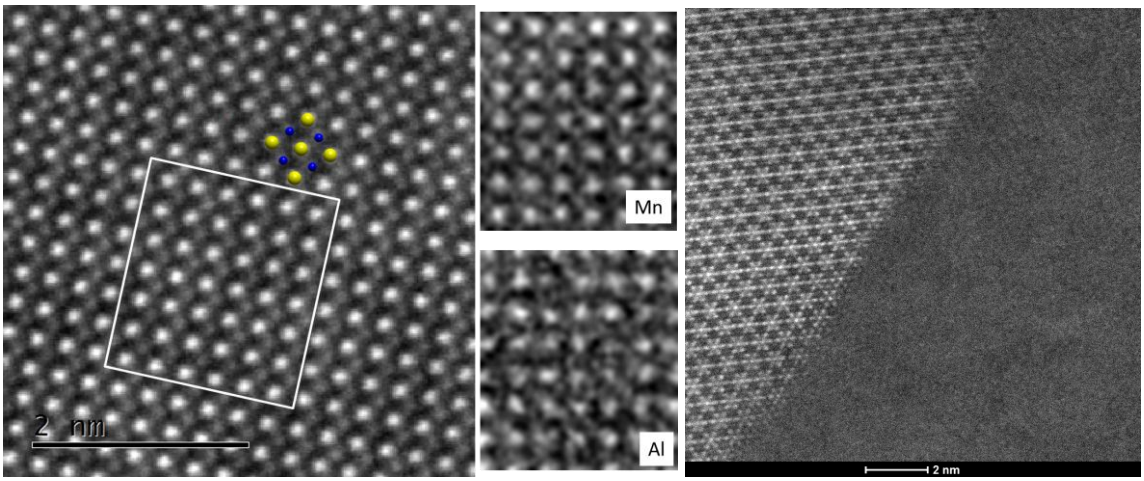

Fig. 4: *HAADF STEM micrographs of the τ-AlMn phase (right, [001] viewing direction) with corresponding model (1x1 unit cell, Mn bright) together with EDS maps of Mn-kAlpha and Al-kAlpha lines (center), grain boundary detail of inclusion and τ-AlMn phase (left).*

3. Conclusions

$Al_{45}Mn_{55}$ ribbons were prepared by rapid quenching; after selection of thermal processing parameters on the basis of results from thermodynamic, kinetic, magnetic, structure and phase analyses it was possible to determine the proper master alloy preparation and optimal heat treatment for maximizing the content of the ferromagnetic τ-AlMn phase.

Chemically resolved scanning transmission electron microscopy analyses on the atomic scale have allowed to verify the local structure of the initial and final phases in thermal processing experiment against atomic models of the respective phases with excellent agreement. In addition, using *in-situ* TEM annealing it was possible to assess the mechanism of formation of the τ-AlMn phase from the original ε-AlMn phase. It was shown by direct observation that the formation of the τ-phase takes place by its nucleation at the ε-phase grain boundaries accompanied by thermally grain growth, in contrast to some notions about its formation by massive transformation. However, certain small amount of so-far unidentified phase other than the ε-phase or τ-phase has been found which exhibit a large number of linear defects and heavily deformed or twinned morphology; the nature and origin of this minority phase will be a subject of further investigations.

Acknowledgement

This work was supported by the project CEKOMAT I, ITMS 26240120006 from the Research and Development Operational Program funded by the ERDF.

References

[1] D. Palanisamy, Ch. Srivastava, G. Madras, K. Chattopadhyay, *J. Mater. Sci.* **52** (2017) 4109–4119.

[2] I. Janotova, P. Svec Sr., P. Svec, I. Matko, D. Janickovic, J. Zigo, M. Mihalkovic, J. Marcin, I. I. Skorvanek, *Journal of Alloys and Compounds* **707** (2017) 137-141.

[3] H. Kono, *J. Phys. Soc. Jpn.* **13** (1958) 1444-1451.

[4] C. Yanar, et al., *Metall. Mater. Trans.* **33A** (2002) 2413-2423.

[5] N. Singh, et al., *J. Alloys Compd.* **633** (2015) 401-407.

[6] I. Janotova et al., this volume.